Virchows Arch (1998) 433:443–447 © Springer-Verlag 1998

ORIGINAL ARTICLE

Tomomi Ihara · Tsukiko Yamamoto
Masao Sugamata · Hiroki Okumura · Yoshio Ueno

The process of ultrastructural changes from nuclei to apoptotic body

Received: 1 April 1998 / Accepted: 22 June 1998

Abstract There have been many reports on the formation of apoptotic bodies, but little is known about the cellular pathological processes and the morphological changes involved. We induced apoptotic cell death by administering nivalenol (NIV), a trichothecene mycotoxin produced by *Fusarium* species, and investigated the ultrastructural process of formation of apoptotic bodies. The thymus was examined by electron microscopy 6, 12, and 18 h after administration. Apoptotic cell death was induced in the thymus of NIV-treated mice. The nuclei became invaginated and pinched off to give fragments, and crescent-shaped spaces (CSS) were found around the nuclear envelopes of these cells at quite an early stage. In some of these spaces, myelin figures were observed. We divided the process of formation into four stages and characterized each of them. These are easily recognized in morphological stages and are also useful for clarifying the apoptotic mechanism.

Key words Apoptosis · Crescent-shaped spaces · Ultrastructure · Nivalenol · Thymus

Introduction

The connection between apoptosis and various phenomena such as aging, development, cancer and immunomodulation, is being elucidated by various methods. Apoptosis is a morphological pattern of cell death characterized by cell shrinkage and increased cell density. The chromatin becomes pyknotic and is compacted into a half-moon shape attached to the nuclear membrane. The nucleus breaks up (observed as karyorrhexis by light microscopy), and the cell appears to bud. The buds often contain pyknotic nuclear fragments and they pinch off to give apoptotic bodies, which are phagocytosed by macrophages or neighbouring cells. During this sequence there is no change in organella [1–4]. Biochemically, internucleosomal DNA cleavage is an early event of cell death associated with apoptosis [5].

The trichothecene mycotoxins, including nivalenol (NIV), which is produced by the *Fusarium* species, are highly cytotoxic to mammalian cells and act by inhibiting protein and DNA syntheses [6–9]. There has recently been a report of karyorrhexis observed in actively growing cells in bone marrow, thymus, and spleen of mice treated with these toxins [10]. On the basis of these reports, we examined whether NIV induces apoptotic cellular damage in vivo [11]. The morphological process of formation or apoptotic bodies in vivo has not yet been described and we induced apoptotic cell death by administration of NIV in order to investigate the ultrastructural process of formation of apoptotic bodies.

T. Ihara · T. Yamamoto · M. Sugamata (✉)
Department of Pathology, Tochigi Institute of Clinical Pathology, 2308-3 Minamiakatsuka, Nogi, Shimotsuga-gun, Tochigi, 329-0112, Japan
Tel.: +81-280-56-1278; Fax: +81-280-56-2792;
e-mail: mspathol@beige.ocn.ne.jp

T. Ihara
Department of Pathology, Omori Hospital, Toho University School of Medicine, 6-11-1 Omori-nishi, Ota-ku, Tokyo, 143-0015, Japan

H. Okumura · Y. Ueno
Department of Toxicology and Microbial Chemistry, Faculty of Pharmaceutical Sciences, Science University of Tokyo, 12 Funagawara-machi, Shinjuku, Tokyo, 162-0826, Japan

Materials and methods

Fusarenon-X (=4-acetyl NIV) isolated from culture filtrate of *Fusarium* species Fn 2B [12] was deacylated into NIV. Female ICR mice purchased from Sankyo Labo Service (Shizuoka, Japan) were used at 5 weeks of age. NIV, dissolved in 0.9% physiological saline, was injected i.p. at a dose of 8.2 mg/kg body weight. Control mice received physiological saline at a dose of 0.1 ml/10 g body weight. Mice were sacrificed under ether anaesthesia 6, 12, and 18 h after the administration. The thymus, fixed in 1% glutaraldehyde-4% formalin over 6 h at 4°C, was rinsed in 0.1 M cacodylate buffer overnight, postfixed in 1% osmium tetraoxide for 1 h at 4°C, and then dehydrated in sequential ethanol series. The fixed tissues were embedded in Epon 812 and sectioned using a Ultratome Nova (LKB, Bromma, Sweden). The sections were double

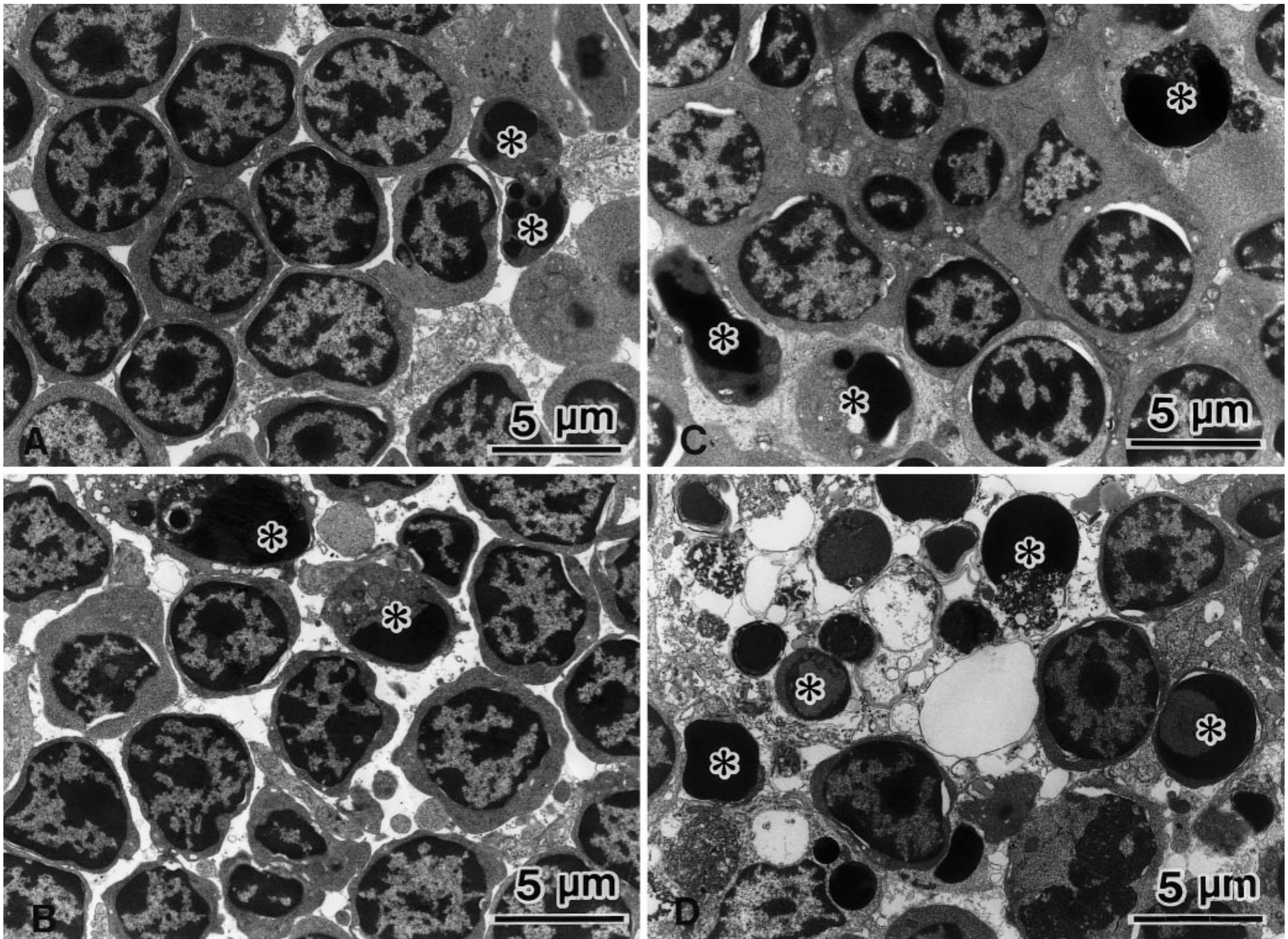

Fig. 1 Electron micrographs of thymus in **A** control mouse and in mice at **B** 6 h, **C** 12 h and **D** 18 h after administration of NIV (general views). Apoptotic thymocytes (*) are observed. ×3,500

stained with uranyl acetate and lead citrate, and were examined under a 1200 EX electron microscope (JEOL, Tokyo). The animal experiment was performed according to the principles of laboratory animal care.

Results

By 6, 12, and 18 h after NIV administration, apoptosis was induced in the thymus; the number of apoptotic cells increased in proportion to the time elapsed after administration. Apoptosis was also observed in controls, but the frequency was strikingly lower than in the test thymuses at 12 h and 18 h after administration. Furthermore, compared with control thymuses, test thymuses 6 h administration of NIV had more abundant invaginations of nuclei, although the frequency of apoptotic cells was similar to that in controls (Fig. 1A–D). In individual thymocytes, when the thymus was examined at 12 h after administration the following findings were observed. Chromatin was irregularly condensed, nuclei were invaginated, nuclear blebs developed and pinched off to form fragments (Fig. 2A–E). Perinuclear spaces, which we call "crescent-shaped spaces" (CSS), were found on these cells, and myelin figures can be observed in some of these spaces (Fig. 2B, inset), which were observed at an early stage of nuclear change (Fig. 2A). Their frequency was much higher in NIV-treated mice than in controls. The nuclear fragments were gradually condensed and compacted into half-moon shapes (Fig. 2F), and apoptotic bodies were formed (Fig. 2G) and phagocytosed by macrophages (Fig. 2H).

Discussion

In Fig. 3 we propose a scheme illustrating the process of ultrastructural change resulting in apoptotic bodies. We have divided the process into four stages and consider that the following findings can be observed at each stage. In stage I the CSS appear around nuclei, remaining as a finding common to all stages. Myelin figures can sometimes be observed in these spaces. Chromatin condenses irregularly. (This stage corresponds to Fig. 2A.) In stage II nuclei invaginate moderately and blebs then appear. (This stage corresponds to Fig. 2B, C.) By stage III the

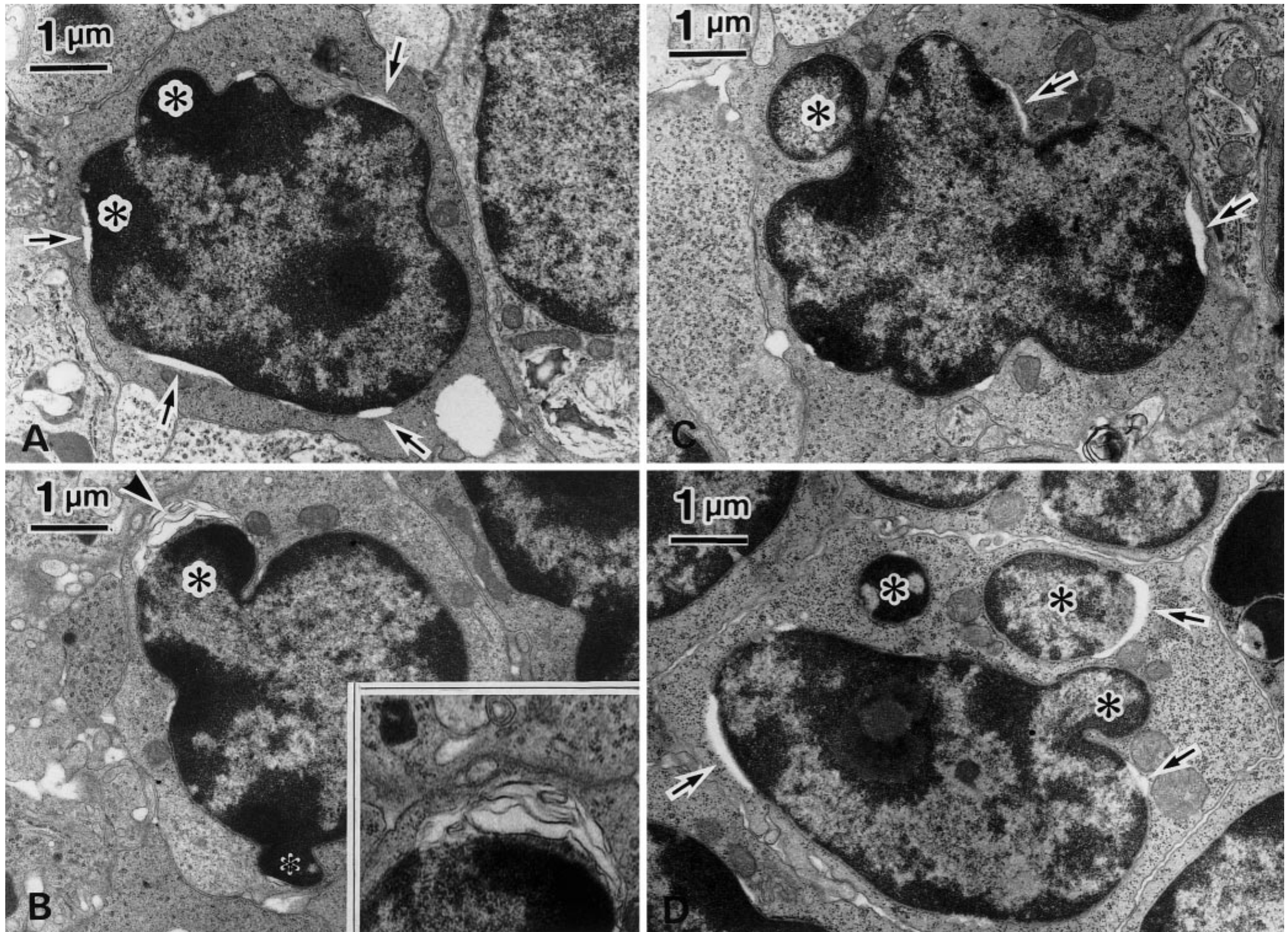

Fig. 2 **A** Crescent-shaped spaces (CSS) appear around the nucleus (*arrow*), which are caused by irregular condensation of chromatin (*). ×9,500 **B** Nucleus invaginates with CSS and nuclear blebs are developing (*). ×9,500 *Inset*. In CSS, the myelin figure appears (*arrowhead*). ×20,000 **C** A nuclear bleb is ready to pinch off (*). *Arrow* indicates CSS. ×9,500 **D** Some blebs have pinched off to fragments (*), and another bleb is developing (*). *Arrow* indicates CSS. ×9,500 **E** Nucleus is pinched off to fragments (*). *Arrow* indicates CSS. ×9,500 **F** Chromatin of fragments is compacted into crescent shapes (*). *Arrow* indicates CSS. ×7,000 **G** Apoptotic bodies are formed (*). ×7,500 **H** Apoptotic bodies (*) are phagocytosed by a macrophage (*M*). ×6,500

nuclear blebs are pinching off to form fragments, and they gradually condense. The cytoplasm also condenses and shrinks. (This stage corresponds to Fig. 2D, E.) In stage IV the chromatin of fragments compacts into half-moon shapes.

Apoptotic bodies are formed and phagocytosed by other cells (macrophages). (This stage corresponds to Fig. 2F–H.) The cells corresponding to each stage of the process were found in all thymuses of NIV-treated mice 6, 12, and 18 h after administration. However, the cells corresponding to stages I and II were observed predominantly 6 h after, and those specific to stage IV, 18 h after.

We consider that the appearance of CSS indicates the start of formation of apoptotic bodies. In vivo, the connection of cells to the interstitium prevents the cytoplasm of apoptotic cells from following the nuclear change immediately. Thus, it is suggested that the spaces that we call CSS appear between nuclei and cytoplasm and are observed more frequently in vivo than in vitro [13]. It is difficult to define the content of CSS by ultrastructural observation: however, myelin figures were observed in some of these spaces, and the contens are considered to have quite a high proportion of lipid to protein.

Our preliminary experiments showed the formation of the CSS in other organs, in addition to which a similar process of formation of apoptotic bodies has been observed with other mycotoxins [14]. We therefore suggest that the cells of many tissues follow the same morphological progression to become apoptotic bodies. However, CSS were also detected in the control thymuses in this study, and it is well known that over 95% of thymocytes die by apoptosis. It is highly likely that there is no great difference between physiological and experimental apoptosis.

The stages are easily recognized and do not require expertise in pathology. In all cases of apoptosis, the

Fig. 2E–H (continued)

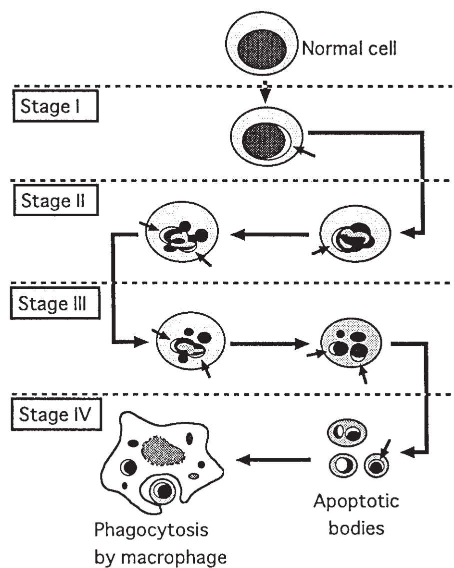

Fig. 3 Diagram representing ultrastructural process of formation of apoptotic bodies. The process is divided into four stages. *Arrow* indicates CSS

progression from a cell in which the process of apoptosis has been triggered to the formation of apoptotic bodies and phagocytosis by macrophages can be observed morphologically. We believe this will aid in the study of the pharmacokinetics and special characteristics of organs.

References

1. Kerr JFR, Wyllie AH, Currie AR (1972) Apoptosis: a basic biological phenomenon with wide-raging implications in tissue kinetics. Br J Cancer 26:236–257
2. Kerr KFR, Harmon BV (1991) Definition and incidence of apoptosis: a historical perspective. In: Tomei LD, Cope FO (eds) Apoptosis: the molecular basis of cell death. Cold Spring Harbor Laboratory Press, Cold Spring Harbor, pp 5–29
3. Tomei LD, Cope FO (1994) Apoptosis: the molecular basis of cell death, vol 2. Cold Spring Harbor Laboratory Press, Cold Spring Harbor
4. Majno G, Joris I (1995) Apoptosis, oncosis, and necrosis: an overview of cell death. Am J Pathol 146:3–15
5. Wyllie AH (1980) Glucocorticoid-induced thymocyte apoptosis is associated with endogenous endonuclease activation. Nature 284:555–556
6. Ohtsubo K, Saito M (1972) Cytotoxic effect of scirpene compounds fusarenon-X produced by *Fusarium nivale*, dihydronivalenol and dihydro-fusarenon-X on HeLa cells. Jpn J Med Sci Biol 23:217–225

7. Ueno Y, Nakajima M, Sakai K, Sato N, Shimada N (1973) Comparative toxicology of trichothecene mycotoxins: inhibition of protein synthesis in animal cells. J Biochem 74:285–296
8. Ueno Y (1991) Biochemical mode of action of mycotoxins. In: Smith JE, Henderson RS (eds) Mycotoxins and animal food. CRC Press, Boca Raton, pp 437–453
9. Terse PS, Mahastha MS, Zurovac O, Stingeffow D, Marquardt RR, Kemppainen BW (1993) Comparison of in vitro and in vivo biological activation of mycotoxins. Toxicon 31:913–919
10. Saito M, Ohtsubo K (1974) Trichothecene toxins of *Fusarium* species. In: Purchase IFH (ed) Mycotoxins. Elsevier, Amsterdam, pp 263–281
11. Sugamata M, Ihara T, Todate A, Okumura H, Yoshino N, Hamaguchi M, Ueno Y (1997) Apoptotic cellular damages in thymus, spleen and liver after nivalenol-induced acute toxicosis in mice: a ultrastructural study. Mycotoxins 45:39–43
12. Ueno Y, Ueno I, Amakai K, Ishikawa Y, Tsunoda H, Ohkubo K, Saito M, Enomoto M (1970) Toxicological approaches to the metabolites of Fusaria... . Isolation of fusarenon-X from the culture filtrates of *Fusarium nivale* Fn 2B. Jpn J Exp Med 41:507–519
13. Ueno Y, Umemori K, Niimi El, Nagata S, Sugamata M, Ihara T, Kawai Kl, Ueno I, Tashiro F (1995) Induction of apoptosis by T-2 toxin and other natural toxins in HL- 60 human promyelotic leukemia cells. Nat Toxins 3:129–137
14. Ihara T, Sugamata M, Sekijima M, Okumura H, Yoshino N, Ueno Y (1997) Apoptotic cellular damage in mice after T-2 toxin-induced acute toxicosis. Nat Toxins 5:141–145